Available online at www.sciencedirect.com
ScienceDirect
Geochimica et Cosmochimica Acta 75 (2011) 106–118
Geochimica et Cosmochimica Acta
www.elsevier.com/locate/gca

Calcium isotopes in a proglacial weathering environment: Damma glacier, Switzerland

Ruth S. Hindshaw [a,b,*], Ben C. Reynolds [a], Jan G. Wiederhold [a,b], Ruben Kretzschmar [b], Bernard Bourdon [a]

[a] Institute of Geochemistry and Petrology, ETH Zurich, Clausiusstrasse 25, 8092 Zurich, Switzerland
[b] Institute of Biogeochemistry and Pollutant Dynamics, ETH Zurich, CHN, Universitätstrasse 16, 8092 Zurich, Switzerland

Received 30 April 2010; accepted in revised form 28 September 2010; available online 8 October 2010

Abstract

The biogeochemical cycling and isotopic fractionation of calcium during the initial stages of weathering were investigated in an alpine soil chronosequence (Damma glacier, Switzerland). This site has a homogeneous silicate lithology and minimal biological impacts due to sparse vegetation cover. Calcium isotopic compositions, obtained by TIMS using a ^{43}Ca–^{46}Ca double spike, were measured in the main Ca pools. During this very early stage of weathering, the young soils which have formed ($\delta^{44/42}Ca = +0.44‰$) were indistinguishable to the rocks from which they were derived ($\delta^{44/42}Ca = +0.44‰$) and stream water ($\delta^{44/42}Ca = +0.48‰$) was also within error of the average rock. This lack of variation indicates that the dissolution of the bulk silicate rock does not strongly fractionate Ca isotopes. The only Ca pool which was strongly fractionated from bulk rock was vegetation, which exhibited an enrichment of light Ca isotopes. Significant Ca isotope fractionation between bulk rock and the dissolved flux of Ca is likely to only occur where the Ca biogeochemical cycle is dominated by secondary processes such as biological cycling, adsorption and secondary mineral precipitation.

1. INTRODUCTION

The weathering of silicate rocks is thought to influence climate change over geological timescales as the reaction of atmospheric CO_2 with silicates releases divalent cations and bicarbonate into rivers which will ultimately form calcium (Ca) or magnesium carbonates in the ocean, resulting in a net removal of CO_2 from the atmosphere (Berner et al., 1983; Walker et al., 1981). Yet the amount of silicate weathering now and in the past is poorly quantified, even though it is an important parameter in modern climate models (e.g. Ludwig et al., 1999). Silicate weathering in the past is typically inferred from proxies such as the strontium isotopic composition of carbonate sediments (Richter et al., 1992). The riverine Ca flux is a key component of the mass balance of Ca in the oceans and is thought to control short term fluctuations in the Ca isotopic composition of the ocean (Farkaš et al., 2007). To understand past fluctuations in the Ca isotopic composition of the ocean one needs to ascertain the modern controls of the riverine Ca isotopic flux. The amount of silicate weathering has been assessed by analysing the dissolved load of the largest rivers draining the world's continents (Meybeck, 1987). This riverine flux will not only consist of silicate sources, but also carbonate and evaporite sources. To distinguish the contribution of each of these sources to the total dissolved ion load, elemental and isotopic ratios are often used (e.g. Gaillardet et al., 1999). However, this calculation is hampered by the fact that the sources can have similar elemental and isotopic compositions, e.g. carbonate rocks can become enriched in radiogenic strontium (Sr) from coexisting silicate rocks during metamorphism (Palmer and Edmond, 1992). To characterise the contribution of silicate rocks, it is necessary to

* Corresponding author at: Institute of Geochemistry and Petrology, ETH Zurich, Clausiusstrasse 25, 8092 Zurich, Switzerland.
E-mail address: hindshaw@erdw.ethz.ch (R.S. Hindshaw).

0016-7037/$ - see front matter © 2010 Elsevier Ltd. All rights reserved.
doi:10.1016/j.gca.2010.09.038

analyse well-defined catchments which only drain silicate lithologies. Here, parameters such as vegetation cover and precipitation are known, allowing the actual silicate weathering process for a specific set of conditions to be studied (White and Blum, 1995; Oliva et al., 2003). This approach has not been without problems since even in granitic catchments, non-silicate minerals such as apatite and calcite may exist (White et al., 1999).

Despite the dominant role of Ca in modulating the carbon cycle and its importance in biogeochemical cycles, the behaviour of Ca has, in the past, been inferred from measurements of Sr isotopes in conjunction with Sr/Ca ratios (e.g. Capo et al., 1998). Strontium was chosen because of its similar chemical behaviour to Ca and the ease with which radiogenic Sr variations can be measured. However, Sr may not always be a suitable analogue for the behaviour of Ca, especially where biological cycling is present (Poszwa et al., 2000). In recent years, however, the techniques have become available which allow the measurement of Ca isotope ratios with suitable precision. Like Sr, Ca can have stable and radiogenic isotopic variations. The radiogenic variations are caused by the decay of ^{40}K to ^{40}Ca, with a decay constant of 5.543×10^{-10}year^{-1} (Steiger and Jäger, 1977). Due to the natural dominance of ^{40}Ca, radiogenic enrichments are relatively small and only old rocks with high K/Ca ratios will show significant enrichment (Marshall and DePaolo, 1982). Thus unlike Sr, where the main applications have used the radiogenic component, Ca isotopic studies have mainly focussed on stable isotope variations (e.g. DePaolo, 2004).

Calcium isotopes have been employed in an increasing number of applications as reviewed by DePaolo (2004), these include: K/Ca dating (e.g. Marshall and DePaolo, 1982), paleo-oceanography (e.g. Farkaš et al., 2007), biological fractionation (Skulan et al., 1997; Bullen et al., 2004; Page et al., 2008; Holmden and Bélanger, 2010), calcite/aragonite precipitation (Gussone et al., 2003; Lemarchand et al., 2004), abiotic fractionation (Ewing et al., 2008) and weathering studies (Schmitt et al., 2003; Wiegand et al., 2005; Tipper et al., 2006, 2008; Cenki-Tok et al., 2009). These previous weathering studies have been conducted in quite complex settings. The studies in the Strengbach catchment (France) (Cenki-Tok et al., 2009) and Hawaii (Wiegand et al., 2005) highlighted the complicated effects of biological cycling and throughfall on Ca isotope ratios in forested ecosystems and the studies in the Himalaya (Tipper et al., 2006, 2008) were conducted in lithologically mixed catchments where secondary precipitation of Ca also occurred. These complex settings made it hard to identify the processes causing the observed Ca isotopic variations.

The objective of this study was to investigate Ca isotopic fractionation during silicate weathering and subsequent biogeochemical cycling by focussing on a lithologically homogeneous alpine catchment with minimal vegetation cover. This simplified the number of potential processes causing isotopic variability. Due to glacial retreat, a soil chronosequence exists in the chosen catchment, allowing both the initial stages of weathering and accompanying soil formation to be studied.

2. STUDY AREA

The Damma glacier is a small (10.7 km^2), glacial catchment situated in the central Swiss Alps (Fig. 1). The glacier itself is temperate and has retreated since records began in this area (1921). Two end moraine bands lie across the forefield which were caused by two periods of advance which ended in 1927 and 1992, respectively (VAW, 2005). Large side moraines are present dating from approximately 1850 (the Little Ice Age) (VAW, 2005). Due to a sharp change in relief, a small piece of glacier has become detached from the main glacier during retreat, referred to as 'dead ice'. The elevation of the catchment ranges from 1800 to 3600 m and the glacier currently covers 40% of the catchment area. The forefield area is typically covered in snow for around 6 months of the year. The average annual temperature is 2.2 °C and the annual precipitation is $\sim$ 2000 mm (recorded at the meteo-station, see Fig. 1).

The catchment is underlain by Central Aar granite: a polymetamorphic basement which was intruded 298 Ma ago by late-Variscan magmatism (the last major thermal event of the region) (Schaltegger, 1994), resulting in an acidic suite of rocks. During Alpine orogeny further metamorphic resetting took place between 20 and 65 Ma (Dempster, 1986) resulting in a greenschist facies. Carbonates have not been detected in any of the rock samples which have been analysed so far (de Souza et al., 2010). The average lithology is: quartz (32%), plagioclase (32%, $An_{0.1}$), microcline (23%), muscovite (5.6%), biotite (3.6%), epidote (2.8%) together with trace amounts of apatite. Biotite was extensively altered to chlorite during Alpine orogeny. Epidote is finely disseminated throughout the rock and could be highly reactive (Mavris et al., 2010; Oliva et al., 2004). Thus, the main Ca bearing minerals are plagioclase, apatite and epidote.

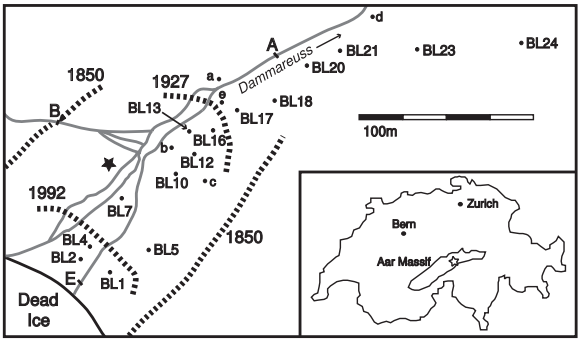

Fig. 1. Map of the sampling locations. The star in the inset shows the location of the Damma glacier in relation to the rest of Switzerland. The numbers in the main map refer to soil sampling locations (the higher the number, the older the site) and the upper case letters mark water sampling locations. Lower case letters are ground water and porewater sampling locations: a = G1, b = G2, c = hm92-1, d = EP2 and e = BR2. The star marks the position of the meteo-station where rain samples were collected and stream discharge was measured at A. Dashed lines represent the moraines with the ages adjacent. The dead ice begins at 2060 m and Site A is at 1940 m, the stream flows in the direction of the arrow.

The whole valley floor is a braided stream system, and the streams are ephemeral. The main stream, the Dammareuss, emanates from the glacier and passes underneath the dead ice. A side stream, which also drains the glacier, cuts through the western side moraine to join the main stream (Fig. 1).

Within the forefield area, the ice-free age (exposure since deglaciation) is known as a result of detailed monitoring, providing a soil chronosequence. This soil chronosequence currently spans approximately 150 years and is around 1.5 km in length. For simplicity, it is assumed that the age of the soil upon exposure is 0, i.e. there is no relict soil from previous glacial retreats and no weathering of the rock underneath the glacier. Soils in the chronosequence overlie bouldery morainal material, are poorly weathered, thin and contain large rock fragments. They were classified as Hyperskeletic Leptosols (Dystric or Eutric) according to the World Reference Base for Soil Resources (WRB, 2006). The transition from Eutric (base saturation $> 50\%$) to Dystric (base saturation $< 50\%$) occurs after $\sim$70 years. There are two discontinuities in this chronosequence due to the periods when the glacier advanced, resulting in three distinct sections of development. The youngest part (exposed since 1992) is characterised by large boulders and glacial debris and only a few pioneer plants. In the middle section (exposed between 1927 and 1950), soils begin to form and plant cover increases dramatically. The plants are typically herbs and grasses (e.g. *Agrostis gigantea* and *Rumex scutatus*). The oldest section (exposed before the early 1900 s) is characterised by the dominance of woody vegetation such as *Rhododendron ferrugineum*.

3. SAMPLING AND ANALYTICAL METHODS

3.1. Sample collection

Soil samples were collected in September 2007 as part of the BigLink project (Bernasconi, 2008). Twenty-one sampling locations (Soils BL1- BL21, of which 13 were analysed for Ca isotopic composition) were chosen by randomly selecting sites within a pre-determined grid. This means that the approximate age was pre-determined but the final location was random, allowing spatial heterogeneity to be accounted for whilst covering the length of the chronosequence. In addition, two older sites which were unaffected by glaciation in the last 150 years (reference sites) were picked which were just outside the forefield (Soils BL23 and BL24). These two soils were classified as Haplic Cambisols (Dystric, Humic, Skeletic) (WRB, 2006). At each of the sampling locations a 50×50 cm frame was placed on the ground and after the removal of above ground vegetation the soil was sampled at depths of 0–5 cm (samples BLXa) and 5–10 cm (samples BLXb). Roots and stones were removed from each sample before sieving at 0.8 cm. Each sampling point was sampled in triplicate and the soils pooled together to provide one sample for each depth at each site. This composite sample was typically 6 kg. The soil was air-dried at 40 °C and sieved at 2 mm before storage. Additional soil samples (described in Electronic annex EA-1) analysed for Ca isotopes were sampled in 2006 (de Souza et al., 2010).

Water samples were collected as part of a larger sampling effort to investigate spatial and temporal variability in the dissolved load. Water samples were collected every two weeks throughout the 2008 melt season (May to October). Samples for cation analysis were filtered in the field through 0.2μm nylon filters into pre-cleaned HDPE bottles and acidified to pH 2. Samples were stored at 4 °C prior to further analysis. Three locations were sampled (Fig. 1): The stream exiting from under the dead ice (site E), the side stream (site B) and the main stream at the gauging station (site A). The majority of the braided channels had converged upstream of the gauging station. Rain samples were collected biweekly from a plastic funnel installed next to the meteo-station. The funnel was covered with thin gauze to prevent insects from flying in. Snow samples were collected using sterile gloves after removal of the top few centimeters of the snow pack. The samples were then allowed to melt naturally. Porewater samples were collected from suction cups installed at depths of 5–25 cm and groundwater samples were collected from two tube wells which reached the water table. Snow, rain, pore and ground water samples were filtered and acidified as described above for stream water samples. Discharge measurements were recorded at Site A using a permanently installed pressure gauge. During collection in May (samples 20080513 A and 20080527 A, Table 4) the pressure gauge was not working, here we estimate the discharge to be 250 and 800 $L\,s^{-1}$, respectively. Sites E and B had pressure gauges installed for part of the summer only.

Leaves from *Rhododendron ferrugineum* were collected during the growing season from an $\sim$ 75 year old site. Each sample is a composite sample of leaves from different specimens.

3.2. Sample preparation

Soil samples were digested using either microwave digestion with concentrated HCl, HNO_3 and HF or by dissolution using the same acids on a hotplate for several days. The procedure for preparing the rock samples and mineral separates is described elsewhere (de Souza et al., 2010). Briefly, rock samples were crushed and then digested identically to the soil samples. Mineral separates of biotite, plagioclase and K-feldspar were obtained by use of heavy liquids, magnetic separation and hand-picking. Leaves were briefly washed with deionized water, dried at 35 °C and ground before digestion using concentrated HNO_3 and 30% H_2O_2. Elemental concentrations of the rocks and soils were determined by X-ray fluorescence spectrometry (XRF) (Spectro X-Lab 2000, Spectro Analytical Instruments, Germany) and elemental concentrations of mineral separates, water and plant samples were analysed by inductively-coupled plasma optical emission spectrometry (ICP-OES) (Vista-MPX, Varian Inc., USA).

Due to potential isobaric interferences (e.g. from double charged Sr) and ionisation inhibition on a TIMS filament, each sample must be purified by ion-exchange chromatography. Previous methods developed for relatively pure samples (Skulan et al., 1997; Schmitt et al., 2003; DePaolo, 2004; Kasemann et al., 2008) were found to be inadequate

for soil and rock samples, due to the higher concentrations of Al and Fe, which partially elute with Ca when using 1–2 M HCl (see Fig. EA-2). Fe and Al impurities have previously been shown to reduce the Ca ion yield and thus beam stability in TIMS measurements (Boulyga, 2010). A four column procedure was thus developed, including the following steps (the full procedure can be found in Electronic annex EA-2):

1. Ca was eluted in 3 M HNO_3 through Eichrom Sr-Spec resin which retained Sr and Ba.
2. Ca was eluted in 6 M HCl through AG-1 X4 anion resin where Fe is retained as $FeCl_4^-$ together with the anion matrix.
3. Al was removed by elution in 0.1 M HF and 1 M HNO_3 through AG50W-X8 cation resin (based on Schiller et al., 2007). Ca is retained and then eluted in 6 M HNO_3.
4. Remaining alkali and alkali earth elements were removed by elution in 1 M HCl through AG50W-X8 cation resin. Ca is retained and then eluted in 2 M HCl.

Three to four micrograms of Ca were processed through column chemistry and the yield was estimated to be 95%. A double spike (^{43}Ca–^{46}Ca) was added before purification so that any fractionation caused by the less than 100% yield was corrected for, in addition to the instrumental mass fractionation, during the TIMS measurement (Russell and Papanastassiou, 1978). The procedural blank through chemical separation was less than 10 ng which is over 300 times smaller than the smallest sample processed.

3.3. Mass spectrometry

All samples were measured by thermal ionisation mass spectrometry (TIMS) (Triton, Thermo Fisher Scientific). Ca (0.7–1 μg) was loaded in nitric form together with 1 μL of Ta phosphate activator solution (Birck and Allègre, 1978) onto degassed rhenium filaments. Samples were run as single filaments in static multicollector configuration utilising the full spread of cups (L4 – ^{40}Ca, L2 – ^{41}K, L1 – ^{42}Ca, H1 – ^{43}Ca, H2 – ^{44}Ca, H4 – ^{46}Ca). ^{41}K was monitored in order to correct for any isobaric interference of ^{40}K on ^{40}Ca. In order to correct for instrumental mass bias, a ^{43}Ca–^{46}Ca double spike was used. The optimal sample to spike ratio was calculated to be 20 (Rudge et al., 2009). This spike pair was chosen since ^{44}Ca and ^{42}Ca are used for normalisation in the calculation of radiogenic anomalies (Russell and Papanastassiou, 1978) and ^{48}Ca cannot be measured at the same time as ^{40}Ca due to the limitation of mass dispersion. Double-spike deconvolution was performed offline following Siebert et al. (2001) and Rudge et al. (2009). Filaments were heated until the smallest beam was greater than 10^{-12} A (typically ^{42}Ca) to minimise baseline errors. Amplifier rotation was employed to cancel out differences in amplifier gains and the baseline was recorded before each run. A run consisted of 28 blocks of 20 cycles with an integration time of 8 s. This was later reduced to 14 blocks when it was observed that the external reproducibility was not affected. Session to session drifts of standard measurements have been reported on TIMS instruments (Krabbenhöft et al., 2009; Simon et al., 2009). We also observed this drift in repeated measurements of SRM 915 b over time (Fig. 2) but corrected for it by 'bracketing' each group of samples on one turret with at least two standards. Due to the limited supply of SRM 915a, SRM 915 b was used as the primary standard. For each turret, the measured SRM 915 b values were averaged and corrected to 0, this same correction was then applied to all samples run on the same turret. This correction varied from −0.20 to +0.14‰. Values are then expressed in standard delta notation:

$$\delta^{\frac{44}{42}}\mathrm{Ca} = 1000\left\{\frac{\left(\frac{^{44}\mathrm{Ca}}{^{42}\mathrm{Ca}}\right)_{\mathrm{sample}}}{\left(\frac{^{44}\mathrm{Ca}}{^{42}\mathrm{Ca}}\right)_{\mathrm{SRM915b}}} - 1\right\} \quad (1)$$

Repeat analyses of SRM 915 b gave $\delta^{44/42}\mathrm{Ca} = 0.01 \pm 0.01$ ($n = 79$, 95% confidence level). For all samples, the $2\sigma_{ext}$ of the standard (0.07) is used as a measure of the external reproducibility. Finally, samples were converted to a delta

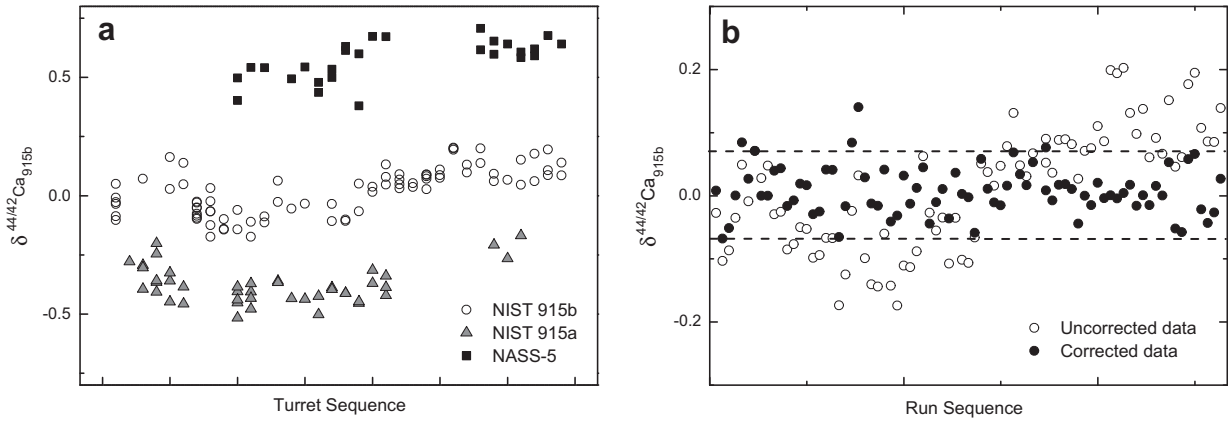

Fig. 2. (a) Long term uncorrected measurements of the three main standards used in this study: 915a, 915b and NASS-5. This illustrates the problem of drift between turrets. (b) The result of the correction applied to 915 b measurements. The correction essentially brackets the samples on each turret using 2 or more standards (see main text for more details). The dashed lines depict the $2\sigma_{ext}$ error of 0.07‰.

Table 1
Sequential extraction procedure for 0.5 g of soil.

Step	Target pool	Reagent	Volume (ml)	T (°C)	Reaction time
1	Exchangeable	1 M NH_4Cl	20	25	16 h
2	Organically bound	H_2O_2/HNO_3	2 × 2.5	85	2 × 1 h
		1 M CH_3COONH_4	15	25	16 h
3	Phyllosilicates	1 M HNO_3	10	180	3 h
4	Residual 1	Aqua Regia	10	120*	1 week*
5	Residual 2	HNO_3/HCl/HF	10		

*Microwave digestion.

value with respect to SRM 915a (+0.35‰) as the use of SRM 915a as the primary standard follows the recommendation by (Eisenhauer et al., 2004). The $\delta^{44/42}$Ca value is used, since unlike $\delta^{44/40}$Ca it is not affected by potential radiogenic enrichments. Although the wide absolute range in measured standard values is reduced by normalising the average of the SRM 915b measurements on each turret to 0 (Fig. 2), the resultant range is still large and thus although samples run in duplicate on the same turret generally reproduce very well, caution should be exercised in drawing conclusions over small differences in samples which have only been measured two or three times. A comparison between our measured standard values and those from other laboratories can be found in Electronic annex EA-3.

Radiogenic ^{40}Ca anomalies are reported in epsilon units: the relative difference of the mass-fractionation corrected ratio and a defined value ($^{40/42}$Ca = 151.029) in parts per ten thousand. The $^{42/44}$Ca normalization ratio is taken to be 0.31221 after (DePaolo, 2004). The average ϵ^{40}Ca for 915 b was -0.5 ± 2.8, 0.3 ± 2.3 for 915a and 0.1 ± 3.7 for seawater (all errors $2\sigma_{SD}$). These latter two values are in agreement with the values published by Amini et al. (2009) and Simon et al. (2009) for those standards.

3.4. Soil sequential extractions

Sequential extractions were performed on the 0–5 cm bulk soil samples. As the upper soil layers are more influenced by organic matter, this fraction was considered more likely to exhibit fractionation between pools than the deeper 5–10 cm layer. A procedure based on Nezat et al. (2007) and Rauret et al. (2000) was used and is summarised in Table 1. Initially, a four stage procedure was used but a fifth step was added since aqua regia was not able to dissolve all of the residual material. Three soils were analysed spanning the complete age range (Soils BL4a, BL17a and BL24a, see Fig. 1). For each soil the procedure was carried out in triplicate (Soil BL17a) or duplicate (Soil BL4a and BL24a) to cover sample heterogeneity and the results were then averaged. After each step the solution was centrifuged, the supernatant stored and the solid residue was carried forward to the next step. During Step 2 hydrogen peroxide was added in small amounts to avoid a violent reaction and the total volume was minimised before adding CH_3COONH_4. In the next two steps (Table 1) the sample was heated with no shaking and in Step 5 a microwave digestion was used. Each supernatant collected was filtered at 0.2 μm using a hand-held filter holder (Swinnex-47, Millipore, US) with a syringe and dried down before being diluted in 2% HNO_3 for elemental analysis by ICP-OES. A procedural blank was also analysed and found to be negligible. Due to incomplete dissolution of target pools, sequential extraction procedures may themselves induce fractionation and phases in addition to the target phase will inevitably be attacked (Wiederhold et al., 2007). We cannot rule out that unintended isotope fractionation occurred but assume that the artificial fractionation effects were negligible.

4. RESULTS

4.1. Rock, soil and mineral separates

Stable $\delta^{44/42}$Ca rock values ranged from +0.35 to +0.54‰ with an average of +0.44‰ (Table 2). This agrees very well with a previous measurement of silicate rock in the Himalayas of +0.45‰ (Tipper et al., 2006). The Aar granite has a Rb–Sr dated intrusion age of 298 Ma (Schaltegger, 1994), so it would be expected that K-feldspar could have acquired a radiogenic anomaly equal to 16.5 epsilon. However, the measured epsilon value was 2.6 (Table 2), which indicated that resetting had occurred (Dempster, 1986). Thus, we could not directly measure specific mineral dissolution by tracing the radiogenic Ca component, due to the young K–Ca age of the rocks and the large errors associated with measuring ϵ^{40}Ca. The high Ca content (Table 2) of the biotite separate is likely due to inclusions of a Ca-rich accessory phase such as epidote or apatite. These were intergrown with the biotite and were thus unable to be separated during hand-picking.

The major element chemistry of the soils is very similar both between the two sampled horizons and compared to bulk rock values (Fig. 3, Table 2). The average isotopic composition of the soil ($\delta^{44/42}$Ca = +0.44‰) remained constant and within error of the range of rock values ($\delta^{44/42}$Ca = +0.35 to +0.54‰) along the 150 year timespan of the chronosequence (Fig. 4). Between the two soil horizons there was no significant isotopic difference (42% probability of 95% significance using a Monte Carlo (MC) t-test with an external reproducibility of 0.07‰, as described in de Souza et al., 2010). The two much older reference sites were not significantly different in Ca isotopic composition from those within the glacier forefield (6% probability of 95% significance, MC t-test), although these soils were depleted in Ca compared to the forefield soils (Fig. 3).

Table 2
Analyses of rock, soil and plant samples. Full soil data is reported in Electronic annex EA-1.

Sample[a]	[Ca] (g/kg)	[Mg]	[Na]	[K]	[Al]	[Ti]	[Sr] (mg/kg)	$\delta^{44/42}$Ca[b] $2\sigma_{ext}$=0.07	ϵ^{40}Ca[b]
Rocks									
R02	14.9	4.03	14.0	30.1	56.8	2.65	247	0.47	−0.8
R03	7.74	9.82	13.9	33.8	66.0	2.67	156	0.35	−1.2
R04	13.1	6.35	15.1	31.8	69.0	2.29	285	0.44	−1.1
R05	3.02	–	16.3	34.6	54.5	0.22	40	0.54	1.9
R06	6.76	10.2	15.3	30.0	65.8	2.53	177	0.36	−1.5
R07	6.88	1.90	14.9	40.4	56.0	0.90	74	0.45	0.1
R08	14.4	7.54	13.8	33.2	67.1	3.30	270	0.47	0.5
Average rock								**0.44**	**−0.3**
Minerals									
R07 Biotite	20.7	16.7	5.02	40.6	43.3	58.1	54	0.50	0.0
R07 Plagioclase	4.95	0.33	31.7	8.03	48.5	0.64	62	0.47	−0.1
R07 K Feldspar	1.00	0.06	20.3	82.8	96.8	0.01	38	0.36	2.6
Soils									
Average 0–5 cm, $n = 20$	10.2	6.05	15.5	27.3	59.3	2.28	175	0.41	0.1
Average 5–10 cm, $n = 14$	9.43	5.62	17.1	28.4	62.2	2.16	177	0.47	−0.7
Average Additional soils, $n = 15$	9.74	8.51	12.8	28.6	58.1	2.35	157	0.44	−0.3
Plants[c]									
RhL_Y_6_08	0.99	1.15	0.02	13.1	0.00	0.00	1	−0.23	2.9
RhL_1M_7_08	4.07	1.44	0.00	7.39	0.02	0.00	5	−0.19	1.3
RhL_2M_8_08	5.93	1.57	0.00	6.04	0.05	0.00	9	−0.22	0.7

[a] Sample labels as given in (de Souza et al., 2010).
[b] Average of 2 measurements except for average soils.
[c] Element contents based on dry weight.

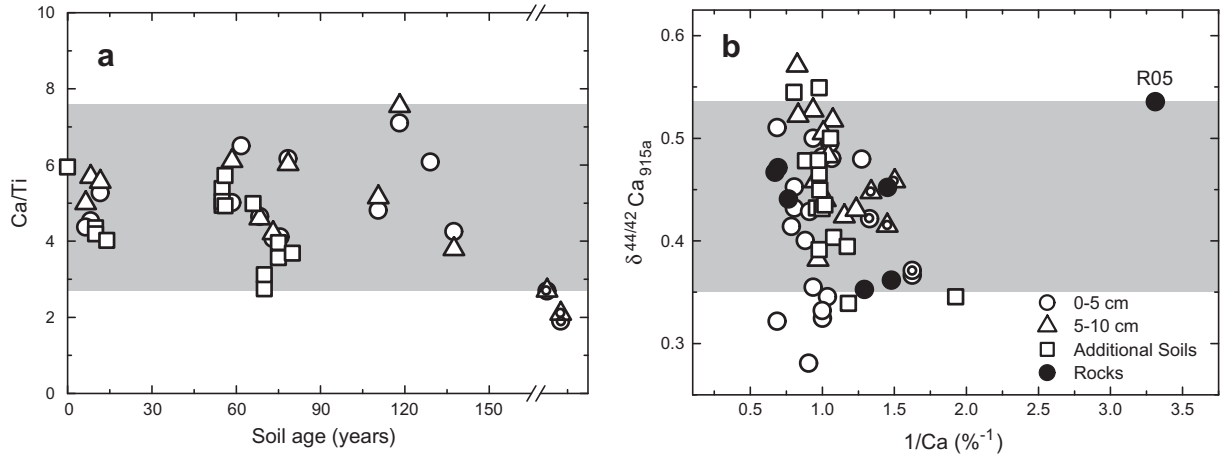

Fig. 3. (a) The Ca/Ti ratio variation over time. This ratio remains constant, only decreasing in the reference soils. The shaded area in both figures represents the corresponding range of rock values (In (a), the Ca/Ti ratio of R05 (13.5) is omitted). (b) Plot of $\delta^{44/42}$Ca against 1/Ca illustrating that although heterogeneous, the isotopic compositions of the soils can be explained by mixing between different rock samples. Rock R05 appears to be an outlier. The reference soils are points marked with internal circles and details about the Additional soils can be found in Electronic annex EA-1.

4.2. Sequential extractions

Bulk soil analyses only yield information about average soil chemical and isotopic compositions, whereas sequential extraction allows different soil pools within the bulk soil to be investigated. Three soils were chosen (0–5 cm depth); a very young soil (Soil BL4a, ~ 10 years old), a soil mid-way down the chronosequence (Soil BL17a, ~ 110 years old) and the reference site (Soil BL24a, > 500 years old).

Table 3 shows that total elemental recoveries, calculated by adding up the amount of each element extracted in each step compared to the bulk soil digest, were for the most part within ±20%. One exception was the recovery of K in Soil 4, this was probably due to an incomplete digest of the bulk

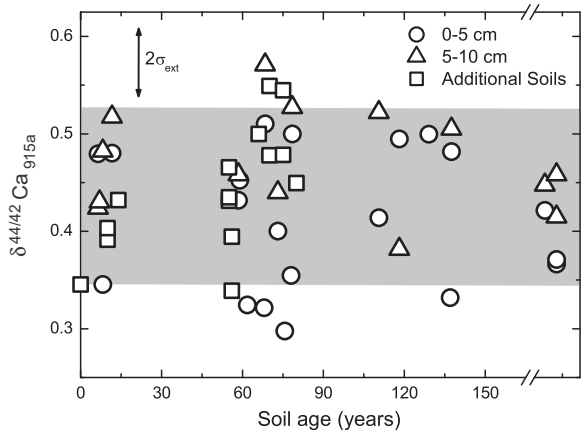

Fig. 4. Ca isotopic composition of the soils as a function of time. Details about the Additional soils can be found in Electronic annex EA-1. The shaded area illustrates the range in $\delta^{44/42}$Ca of the rock.

soil. A ternary plot with Ca, Mg and Na + K at the vertices reveals how closely the extraction procedure reached the target pools, and highlights the variability between soils of different ages (Fig. 5).

Calcium was the most dominant cation in the small exchangeable pool. This pool increased in size for Ca from 1–2 to 5% in 100 years. The organically bound fraction (Step 2) contained nearly 20% of the Ca along with phosphate and so it is likely that this step is dissolving apatite or organically bound P and Ca. Magnesium and Fe were also released, possibly indicating dissolution of secondary (hydr)oxides. Step 3 attacked phyllosilicates (biotite, chlorite) and this extraction step exhibited the highest concentrations of Mg and Fe, for which the main host minerals in this catchment were biotite and chlorite. Where there were five steps in the procedure, it is clear that the fourth step has not been able to fully break down the most resistant silicates - feldspars and plagioclase. It was only with the use of HF in the microwave digest that the residual phase was totally dissolved, releasing large amounts of Na and K as the most resistant minerals dissolved. The aqua regia dissolution (Step 4) was, however, where the highest concentrations of Ca were found.

The isotopic values of the individual sequential extraction fractions can be summed using the formula below and compared to the bulk soil digest isotopic value to check for isotopic mass balance.

$$\delta^{44/42}Ca_{sum} = \sum_{i=1}^{n} f_{Ca,i}\delta^{44/42}Ca_i \quad (2)$$

where i was the sequential extraction step of n steps, $f_{Ca,i}$ was the fraction of Ca extracted in step i and $\delta^{44/42}Ca_i$ was the $\delta^{44/42}$Ca value of the extracted fraction. Assuming that the error on $\delta^{44/42}$Ca dominates (0.07‰) this leads to a combined error of 0.16‰ for the 5-step procedure. Thus, the bulk soil digest Ca isotopic values are within error of

Table 3
Elemental and Ca isotopic compositions of soil sequential extractions.

Sample	Age (years)	Extraction Step	[Ca] (mmol/kg)	[P]	[Mg]	[Fe]	[Na]	[K]	Ca fraction of soil (%)	$\delta^{44/42}$Ca[1] $2\sigma_{ext} = 0.07$
BL4a-1	12	1	2.49	0.17	0.42	0.09	0.09	0.45	1	0.29
		2	30.4	**13.6**	13.6	14.3	0.60	3.18	17	0.39
		3	16.3	5.44	**120**	**137**	1.77	67.9	9	0.57
		4	**117**	0.12	34.2	67.9	1.27	39.0	66	0.41
		5	11.9	0.07	2.38	40.7	**817**	**532**	7	0.60
		sum	*178*	*19*	*170*	*260*	*821*	*642*		*0.43*
BL4a-2	12	1	2.73	0.02	0.50	0.11	0.45	0.95	2	0.40
		2	30.5	**14.4**	17.1	19.2	0.67	3.97	17	0.44
		3	14.1	2.16	**114**	**128**	2.03	64.3	8	0.63
		4	**123**	0.04	34.2	67.6	1.49	43.5	68	0.42
		5	10.6	0.05	1.85	36.7	**740**	**521**	6	0.47[b]
		sum	*181*	*17*	*168*	*252*	*745*	*634*		*0.45*
BL4a	12	bulk	197	12	143	210	886	353		0.48
BL17a-1	111	1	3.12	0.15	1.90	0.34	0.36	1.22	5	0.28
		2	34.3	**20.7**	4.12	11.6	0.98	1.64	15	0.48
		3	2.98	1.38	57.8	52.4	1.22	23.6	9	0.45
		4	**160**	0.40	**129**	**184**	**1064**	**614**	71	0.51
		sum	*201*	*23*	*193*	*248*	*1066*	*640*		*0.49*
BL17a	111	bulk	165	23	227	281	1234	541		0.41[a]
BL24a-1	> 500	1	4.67	0.42	2.70	0.45	1.01	4.74	5	0.42[a]
		2	2.58	24.6	18.8	44.0	0.13	1.79	3	0.31
		3	5.26	**25.6**	**96.8**	**143**	1.09	24.4	5	0.37
		4	**100**	1.50	42.9	80.5	2.69	80.7	81	0.47
		5	10.3	0.32	12.5	47.3	**556**	**379**	7	0.40
		sum	*123*	*52*	*174*	*315*	*561*	*490*		*0.45*
BL24a	> 500	bulk	138	43	158	288	893	408		0.37

Bold type indicates in which fraction the element was most concentrated.
[1] Average of $n = 2$ unless otherwise indicated [a]$n = 1$ [b]$n = 4$.

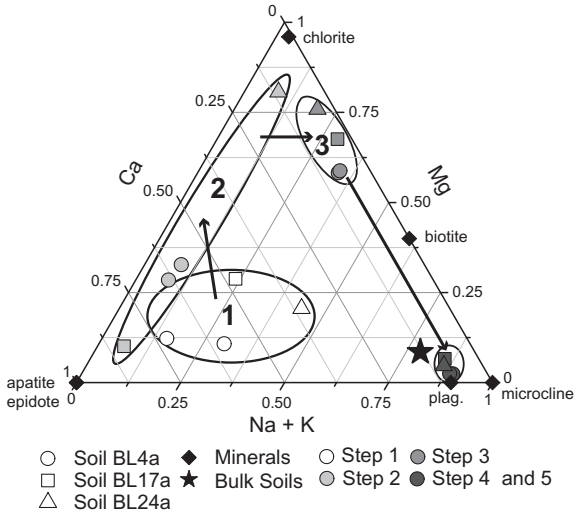

Fig. 5. Ternary plot of the sequential extraction data using normalised molar concentrations. To allow comparison with Soil BL17a the last two extraction steps for the other soils are combined. Soil BL4a was analysed twice and the three bulk soils plot in the same place so only a single point is observed. Soil BL24a (reference site) is clearly different from the other two soils with respect to the first two steps.

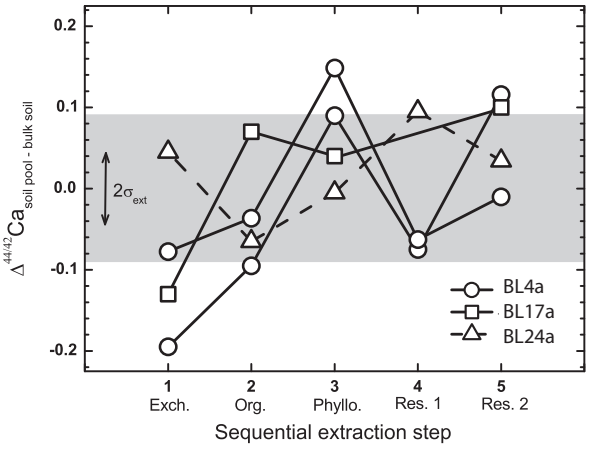

Fig. 6. Ca isotope composition of the different sequential extraction steps (see Table 1) for three different soils. In order to compare the sites, all were normalised to the bulk soil isotopic composition of that site. The sequential extraction procedure was carried out in duplicate for Soil BL4a. Values are reported as $\Delta Ca_{soil\ pool\text{-}bulk\ soil}$ (where the soil pool is a particular sequential extraction step e.g. exchangeable) and the combined external error is indicated. The shaded area highlights the region within which the points are within error of the bulk soil.

those calculated using the above formula. For the two soils in the main chronosequence (BL4a and BL17a), $\delta^{44/42}Ca$ values were lower than bulk soil in the first extraction step (exchangeable pool). In Soil BL4a there was a pronounced increase in $\delta^{44/42}Ca$ from the first to the third extraction step (Fig. 6). There was no significant variation between the different pools extracted in Soil BL24a (reference site).

4.3. Water samples

The Ca isotope values of the stream water at all three sites remained essentially constant, with an average value of $\delta^{44/42}Ca = +0.48‰$ and with no obvious seasonal variation, whilst the Ca flux displayed large seasonal changes (Fig. 7). The Ca isotopic composition of the water samples was not significantly different from that of the soils (29% probability of 95% significance, MC *t*-test) (Fig. 8). However, taken on its own, the 24th June sample exhibited a significantly heavier (76% probability of 95% significance, MC *t*-test) isotopic composition compared to the soils (Fig. 7). Snow samples had lower Ca concentrations and larger $\delta^{44/42}Ca$ values compared with rainwater samples (Table 4). Snow and rainwater isotopic values were similar to (Cenki-Tok et al., 2009). This is to be expected since the study areas are geographically close.

4.4. Plants

Leaf samples from *Rhododendron ferrugineum* were enriched in light Ca isotopes compared to bulk soil (Fig. 8, Table 2), the exchangeable pool (Table 3) and the porewaters (Table 4). This yielded a $\Delta^{44/42}Ca_{leaf\text{-}bulk\ soil}$ of $\approx -0.64‰$. The preferential uptake of light Ca by plants is in agreement with previous studies (e.g. Wiegand et al., 2005). The Ca isotopic composition of plants in this forefield was investigated in more detail during a separate study.

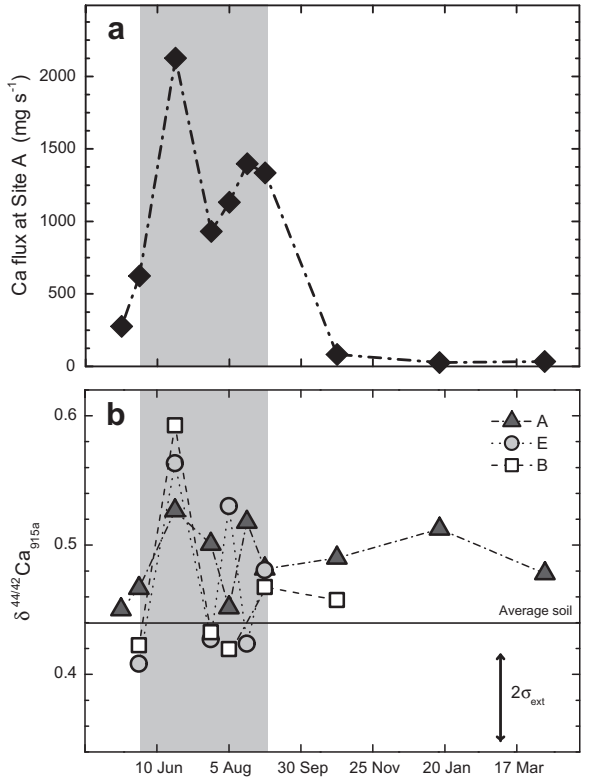

Fig. 7. (a) Calcium flux at Site A. The shaded area in both graphs marks the main melt season. (b) Isotopic composition of the three stream water sampling sites (see Fig. 1) as a function of time. Average soil Ca isotopic composition is marked for comparison.

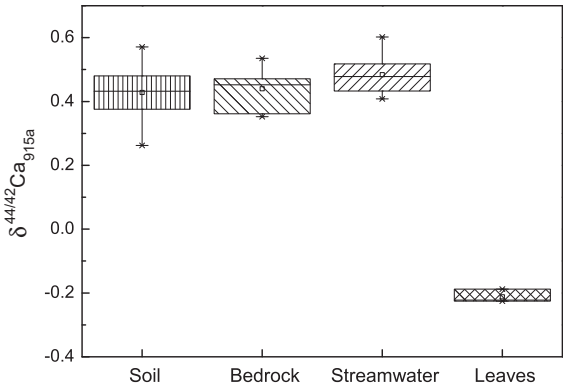

Fig. 8. Box plot summarising the main pools of calcium analysed. Leaves are from *Rhododendron ferrugineum*. This is the only significantly fractionated bulk pool of Ca in the forefield.

5. DISCUSSION

5.1. Weathering in soils

This field site contains young soils (Hyperskeletic Leptosols), which are poorly developed. The chemical index of alteration $(Al_2O_3/(Al_2O_3 + CaO + Na_2O + K_2O))$ of the soils (0.62) was identical to that of the rocks (0.61) and ratios of mobile to immobile elements indicated lack of significant leaching from the soils (Fig. 3a). Secondary clay formation resulting from weathering was only detectable by X-ray diffraction (XRD) analysis at the sites older than ~ 100 years. Earlier formation of small quantities of clay, poorly crystalline secondary phases which are not detectable by XRD, or the alteration of rocks without formation of secondary phases (Miller and Drever, 1977) could not be

Table 4
Calcium isotopic composition and concentration data of the water samples.

Site	Date (YMD)	Discharge[1] ($L s^{-1}$)	[Ca] ($\mu g L^{-1}$)	Flux $mg s^{-1}$	$\delta 44/42Ca$[2] $2\sigma_{ext} = 0.07$
Stream water					
A	20080513	*250*	1103	276	0.45
A	20080527	*800*	780	624	0.47
A	20080624	4502	472	2126	0.53
A	20080722	1908	487	930	0.50
A	20080805	3595	315	1133	0.45
A	20080819	4110	340	1398	0.52[b]
A	20080902	4221	316	1335	0.48
A	20081028	84	974	82	0.49
A	20090116	30	1357	27	0.51
A	20090408	30	1694	34	0.48
B	20080527		641		0.42
B	20080624		439		0.59[a]
B	20080722	421	442	186	0.43
B	20080805	2092	262	549	0.42
B	20080902	2078	267	555	0.47
B	20081028		762		0.46
E	20080527		800		0.41
E	20080624		442		0.56
E	20080722	892	414	369	0.43
E	20080805	1866	295	551	0.53
E	20080819	1083	413	447	0.42
E	20080902	723	440	318	0.48
Groundwater					
G1	20080930		931		0.58
G1	20080930[3]		931		0.48
G2	20080930		1999		0.45
Porewater					
hm92-1			6092		0.45[a]
EP2			3018		0.46
BR2			18132		0.31
Precipitation					
rain	20080708		508		0.46
rain	20080916		662		0.36
rain	20080930		768		0.36
snow	20080513		87		0.49
snow	20081028		248		0.58

[1] Discharge data in italics is estimated where possible (see text).
[2] Average of $n = 2$ unless otherwise indicated, [a]$n = 1$ [b]$n = 3$[3] repeat.

ruled out. The isotopic composition of the soils are determined by mixing between slightly different initial rock compositions without significant mass dependent fractionation (Fig. 3). The coincidence of soil and rock $\delta^{44/42}$Ca values was also reported in the Himalaya (Tipper et al., 2006).

In order to gain more information about the potential sources of Ca to the dissolved load we performed sequential extractions on bulk soils. The largest soil pool of Ca is in the residual fraction which is dominated by plagioclase and feldspar (Fig. 5). There is no decrease in the Ca concentration of this resistant fraction over time, indicating that these Ca rich phases are not yet significantly affected by weathering (even in the reference soil, BL24). When the dissolution of the residual phase was split into two steps, the highly resistant silicates, sodic plagioclase and microcline, did not appear to break down until Step 5, as indicated by the high concentrations of Na and K (Table 3). Although the plagioclase composition is close to that of the albite endmember, it is known that plagioclases exhibit zoning with Ca and Na rich parts and that the Ca rich endmember is more easily weathered (Oliva et al., 2004). Thus, the high concentrations of Ca in Step 4 could stem from a calcic plagioclase (anorthite) or epidote. An extended X-ray absorption fine structure (EXAFS) spectroscopy study on Fe in the forefield found that the Fe fraction within epidote remained constant over the chronosequence, indicating lack of epidote weathering (Kiczka-Cyriac, 2010). This finding, together with the fact that at pH 5 the weathering rate of anorthite is several orders of magnitude faster than that of epidote (Lasaga, 1994), suggests that anorthite is being released in Step 4 with Step 5 dissolving albite and epidote. The apparent stability of epidote in these soils is in contrast to a recent study, based on XRD data, which reported a rapid decrease of epidote content over a 150 year time period in a similar alpine chronosequence (Mavris et al., 2010).

The 'organically bound' fraction (Step 2, Table 3) comprised the second largest pool of Ca in the two forefield soils. These sites contain little organic matter (Smittenberg et al., 2009), thus we do not think that the Ca is predominantly bound to organic matter. Rather, the dominance of P and Ca in this fraction, strongly points to the influence of apatite dissolution. Soil BL17a released Ca and P identical in proportion to the ratio in apatite (5:3), whilst BL4a released slightly more Ca than expected based on congruent apatite weathering. Laboratory experiments have shown that during initial apatite dissolution, weathering is incongruent, resulting in higher initial Ca/P ratios (Valsami-Jones et al., 1998). The absence of Ca in the second extraction step at BL24a could indicate that all the apatite has been weathered and the Ca has been removed, either by leaching or by plant uptake (Blum et al., 2002). Apatite depletion has previously been reported in young soils (Nezat et al., 2008 and references therein) and could provide a vital source of Ca for plants at the youngest sites. A pure sample of apatite from our fieldsite to compare with the isotopic composition of this extraction step could not be obtained, but based on the isotopic composition of this extraction step we would expect the isotopic composition of apatite to be similar to whole rock values. Thus, we do not expect the weathering of apatite to shift the $\delta^{44/42}$Ca value of the exchangeable pool away from that of the residual soil pool.

5.2. Porewaters and the exchangeable pool

Rapid equilibration between porewaters and the exchangeable pool is often assumed to occur (Drever, 1997) and would result in identical $\delta^{44/42}$Ca values in these two pools. Although only three porewater values were measured, it is clear that spatial heterogeneity exists (Table 4). A comparison can be made between the porewater BR2 and Soil BL17 which were located within 50 m of each other; the $\delta^{44/42}$Ca values were +0.28‰ (exchangeable) and +0.31‰ (porewater). Both values are lower than bulk soil ($\delta^{44/42}$Ca at Site BL17 is +0.41‰). It is, nevertheless, hard to tell whether porewater $\delta^{44/42}$Ca controls the exchangeable pool or vice versa, or indeed whether it is realistic to assume that spatial homogeneity exists on this scale. Whichever scenario is assumed, a pool of light Ca is present at the inception of soil formation.

The small size of Ca in the exchangeable pool (1–5% of the total soil Ca) could make it susceptible to external inputs or vegetation. The $\delta^{44/42}$Ca of precipitation (dry and wet combined) measured at this site was identical to the $\delta^{44/42}$Ca of rocks and soils, thus if there is an effect of precipitation on the exchangeable pool it will be hard to observe. Vegetation could potentially control porewater and exchangeable $\delta^{44/42}$Ca values (Holmden and Bélanger, 2010; Bullen et al., 2004). At Damma, fractionation of the exchangeable pool or porewaters is unlikely to be caused by vegetation, since the size of the Ca biomass pool in the glacier forefield is, on average, only $\sim 2\%$ of the size of the exchangeable Ca pool in the 0–5 cm soil layer.

Low $\delta^{44/42}$Ca values of the exchangeable fraction (Step 1, Fig. 6) could be explained by the preferential adsorption of light Ca by soil components. The $\Delta^{44/42}Ca_{\text{soil pool-bulk soil}}$ of the exchangeable fraction increased from BL4a to BL24a (Fig. 6). We use cation exchange capacity (CEC) measured using 1 M NH_4Cl as a proxy for the number of sorption sites available. From BL4a to BL24a the size of the exchangeable Ca pool increases by 250% (Table 3) and the CEC increases by 850% (6.4–59.1 $mmol_c kg^{-1}$), representing an increase in organic matter and clay minerals. Thus, with increasing soil age, there will be a greater variety of sorption sites available. Different sorption sites (e.g. organic vs. mineral) could potentially have different fractionation factors (Lemarchand et al., 2005) and this could change the $\Delta^{44/42}Ca_{\text{exchangeable-bulk soil}}$ depending on which sites Ca sorbs to.

5.3. Stream water

The similarity of the stream water Ca concentration and $\delta^{44/42}$Ca to rain water (Table 4) could potentially be due to the stream being dominated by rain water. The Ca isotopic composition of the precipitation was not constant throughout the year. In particular, snow has a higher $\delta^{44/42}$Ca value (average = +0.53‰) than rain (average = +0.39‰) and is closer to the seawater composition ($\delta^{44/42}$Ca = +0.96‰). The percentage contribution of precipitation (rain, snow

and ice melt) to Ca in the river was calculated using a hydrograph separation model for a neighbouring catchment (Verbunt et al., 2003) combined with a conventional chloride correction using concentrations measured in the Damma catchment. This contribution varied from 2% in the winter months to nearly 35% at the height of summer. Although this correction reduced absolute Ca concentrations, $\delta^{44/42}$Ca values remained, within error, unchanged. Thus, the isotopic composition of rain is close enough to that of the silicate rock in this catchment to not affect the resultant Ca isotopic composition of the river.

The average $\delta^{44/42}$Ca of the stream was, within error, identical to soils and rocks (Fig. 8) indicating that no significant fractionation occurred during the dissolution of primary silicate minerals. The calcium isotopic composition of the stream showed no significant correlation with discharge at Site A, in agreement with the results of Cenki-Tok et al. (2009) and Holmden and Bélanger (2010), even though Ca concentrations varied by a factor of five over the season.

The heaviest dissolved Ca isotopic compositions, coincident at all three sampling sites, were recorded on 24th June when the discharge reached its maximum after the snowmelt period. Increased snowmelt contribution was invoked to explain the highest $\delta^{44/42}$Ca value recorded in the Strengbach catchment (Cenki-Tok et al., 2009). The high $\delta^{44/42}$Ca value of these water samples could be caused by (1) the isotopic composition of the snow itself, (2) snow melt flushing out biological degradation products or (3) snow melt flushing out a pool influenced by secondary processes.

If we assume that 'old' snow contributes most to the isotopic composition of snowmelt, then spring snow melt with the May Ca isotopic composition, which is similar to rock, cannot be the cause of the high $\delta^{44/42}$Ca value observed on 24th June.

Alternatively, snow melt could be flushing out a pool of heavy Ca, which had not been in contact with baseflow during the winter. This pool could be due to biological degradation products which have accumulated over the winter (Clow and Mast, 2010). However, as previously stated, biological control is unlikely due to the small size of the biological pool. Degrading organic matter would be expected to return light Ca back into the system (since plants are isotopically lighter than bulk soils, Table 2), resulting in a decrease in $\delta^{44/42}$Ca during snowmelt which is opposite to that observed.

We favour the third explanation: that secondary processes, namely adsorption (including ion exchange), induced by winter hydrology could cause increased $\delta^{44/42}$Ca values which are then flushed out during snowmelt. In winter, when the vast majority of channels freeze, isolated pockets of water could develop high $\delta^{44/42}$Ca values due to preferential sorption of light Ca onto soil components and when discharge and channel connectivity increase during snowmelt the residual heavy Ca is flushed out. In summer, the braided channel network ensures continual flushing occurs and prevents isolated pockets of water forming.

Sorption of light Ca onto soil components is, as far as we are aware, not yet documented but fractionation during adsorption has been observed for several other stable isotope systems (Balistrieri et al., 2008; Juillot et al., 2008; Mikutta et al., 2009). The seasonal precipitation and dissolution of secondary mineral phases (to which Ca could adsorb) has previously been reported in an alpine catchment (Clow and Drever, 1996). Detailed laboratory and field studies are needed to investigate Ca isotope fractionation during adsorption. Similar hydrological control of the isotopic composition of river waters might be applicable to other climates where there are large seasonal variations in water discharge. There are very few seasonal stream water Ca isotopic studies but comparison of high and low stages of monsoonal rivers reveals that there is likely also a seasonal trend in these large rivers (Tipper et al., 2010).

6. CONCLUSIONS

In this very young weathering environment (0–150 years), no fractionation of Ca isotopes was observed in bulk soil or stream waters compared to the bedrock. Pore and ground waters sampled in the forefield were also unfractionated with respect to bulk rock values. No seasonal variation was observed in the stream, but the hydrological event of snowmelt had a transient impact on streamwater $\delta^{44/42}$Ca, which could be due to seasonal adsorption of Ca. Investigation of the soil pools by sequential extraction indicated that the exchangeable pool is fractionated compared to the parent soil, but the mechanisms causing this are not yet fully understood. Vegetation was significantly enriched in light Ca but vegetal biomass is not yet significant enough to have induced a measurable fractionation on the soils and waters of the catchment.

Our observations imply that Ca isotopes can only become fractionated during silicate weathering if secondary processes are involved (e.g. uptake by vegetation). In future, it will be essential to determine whether such secondary processes play an important role in determining the riverine Ca isotope flux to the world's oceans.

ACKNOWLEDGEMENT

The authors thank Gregory de Souza, Mirjam Kiczka-Cyriac, Emmanuel Lemarchand and Ed Tipper for field sampling and discussions, Martin Imseng for help with developing the sequential extraction method, and the rest of the BigLink project team members for sampling support. The authors would also like to thank Matt Fantle, two anonymous reviewers and Derek Vance for comments which significantly improved an earlier version of this manuscript. This work was associated with the BigLink project of the Competence Center Environment and Sustainability of the ETH Domain (CCES) and was funded by ETH Research Grant No. 04/06-3.

APPENDIX A. SUPPLEMENTARY DATA

Supplementary data associated with this article can be found, in the online version, at doi:10.1016/j.gca.2010.09.038.

REFERENCES

Amini M., Eisenhauer A., Böhm F., Holmden C., Kreissig K., Hauff F. and Jochum K. P. (2009) Calcium isotopes ($\delta^{40/44}$Ca) in MPI-DING reference glasses, USGS rock powders and various rocks: evidence for Ca isotope fractionation in terrestrial silicates. *Geostand. Geoanal. Res.* **33**, 231–247.

Balistrieri L. S., Borrok D. M., Wanty R. B. and Ridley W. I. (2008) Fractionation of Cu and Zn isotopes during adsorption onto amorphous Fe(III) oxyhydroxide: experimental mixing of acid rock drainage and ambient river water. *Geochim. Cosmochim. Acta* **72**, 311–328.

Bernasconi S. M.and BigLink Project Members (2008) Weathering, soil formation and initial ecosystem evolution on a glacier forefield: a case study from the Damma Glacier, Switzerland. *Mineral. Mag.* **72**, 19–22.

Berner R. A., Lasaga A. C. and Garrels R. M. (1983) The carbonate–silicate geochemical cycle and its effect on atmospheric carbon dioxide over the past 100 million years. *Am. J. Sci.* **283**, 641–683.

Birck J. L. and Allègre C. J. (1978) Chronology and chemical history of the parent body of basaltic achondrites by the ^{87}Rb–^{87}Sr method. *Earth Planet. Sci. Lett.* **39**, 37–51.

Blum J. D., Klaue A., Nezat C. A., Driscoll C. T., Johnson C. E., Siccama T. G., Eagar C., Fahey T. and Likens G. E. (2002) Mycorrhizal weathering of apatite as an important calcium source. *Nature* **417**, 729–731.

Boulyga S. (2010) Calcium isotope analysis by mass spectrometry. *Mass Spec. Rev.* **29**, 685–716.

Bullen, T. D., Fitzpatrick, J. A., White, A. F., Schulz, M. S., Vivit, D. V., 2004. Calcium stable isotopic evidence for three soil calcium pools at a granitoid chronosequence. In: *Water-Rock Interaction. Proceedings of the Eleventh International Symposium on Water-Rock Interaction Saratoga Springs, New York*, (eds. R. B. Wanty and R. R. Seal II). Taylor & Francis, London, vol.1, pp. 813–817.

Capo R. C., Stewart B. W. and Chadwick O. A. (1998) Strontium isotopes as tracers of ecosystem processes: theory and methods. *Geoderma* **82**, 197–225.

Cenki-Tok B., Chabaux F., Lemarchand D., Schmitt A.-D., Pierret M.-C., Viville D. and Stille P. (2009) The impact of water–rock interaction and vegetation on calcium isotope fractionation in soil and stream waters of a small, forested catchment (the Strengbach case). *Geochim. Cosmochim. Acta* **73**, 2215–2228.

Clow D. W. and Drever J. I. (1996) Weathering rates as a function of flow through an alpine soil. *Chem. Geol.* **132**, 131–141.

Clow D. W. and Mast M. A. (2010) Mechanisms for chemostatic behaviour in catchments: implications for CO_2 consumption by mineral weathering. *Chem. Geol.* **269**, 40–51.

de Souza G., Reynolds B., Kiczka M. and Bourdon B. (2010) Evidence for mass-dependent isotopic fractionation of strontium in a glaciated granitic watershed. *Geochim. Cosmochim. Acta* **74**, 2596–2614.

Dempster T. J. (1986) Isotope systematics in minerals: biotite rejuvenation and exchange during Alpine metamorphism. *Earth Planet. Sci. Lett.* **78**, 355–367.

DePaolo D. J. (2004) Calcium isotopic variations produced by biological, kinetic, radiogenic and nucleosynthetic processes. In *Geochemistry of Non-traditional Stable Isotopes, Reviews in Mineralogy and Geochemistry*, (eds. C. M. Johnson, B. L. Beard and F. Albarède). Mineralogical Society of America, Washington, DC, vol. 55, pp. 255–288.

Drever J. I. (1997) *The Geochemistry of Natural Waters*, 3rd ed. Prentice-Hall, Upper Saddle River, NJ.

Eisenhauer A., Nägler T. F., Stille P., Kramers J., Gussone N., Bock B., Fietzke J., Hippler D. and Schmitt A.-D. (2004) Proposal for international agreement on Ca notation resulting from discussions at workshops on stable isotope meaurements held in Davos (Goldschmidt 2002) and Nice (EGS-AGU-EUG 2003). *Geostand. Geoanal. Res.* **28**, 149–151.

Ewing S., Yang W., DePaolo D. J., Michalski G., Kendall C., Stewart B., Thiemens M. and Amundson R. (2008) Non-biological fractionation of stable Ca isotopes in soils of the Atacama Desert, Chile. *Geochim. Cosmochim. Acta* **72**, 1096–1110.

Farkaš J., Böhm F., Wallmann K., Blenkinsop J., Eisenhauer A., van Geldern R., Munnecke A., Voigt S. and Veizer J. (2007) Calcium isotope record of Phanerozoic oceans: implications for chemical evolution of seawater and its causative mechanisms. *Geochim. Cosmochim. Acta* **71**, 5117–5134.

Gaillardet J., Dupré B., Louvat P. and Allègre C. J. (1999) Gobal silicate weathering and CO_2 consumption rates deduced from the chemistry of large rivers. *Chem. Geol.* **159**, 3–30.

Gussone N., Eisenhauer A., Heuser A., Dietzel M., Bock B., Böhm F., Spero H., Lea D. W., Bijma J. and Nägler T. F. (2003) Model for kinetic effects on calcium isotope fractionation (δ^{44}Ca) in inorganic aragonite and cultured planktonic foraminifera. *Geochim. Cosmochim. Acta* **67**, 1375–1382.

Holmden C. and Bélanger N. (2010) Ca isotope cycling in a forested ecosystem. *Geochim. Cosmochim. Acta* **74**, 995–1015.

Juillot F., Maréchal C., Ponthieu M., Cacaly S., Morin G., Benedetti M., Hazemann J. L., Proux O. and Guyot F. (2008) Zn isotopic fractionation caused by sorption on goethite and 2-Lines ferrihydrite. *Geochim. Cosmochim. Acta* **72**, 4886–4900.

Kasemann S. A., Schmidt A. N., Pearson P. N. and Hawkesworth C. J. (2008) Biological and ecological insights into Ca isotopes in planktic foraminifers as a paleotemperature proxy. *Earth Planet. Sci. Lett.* **271**, 292–302.

Kiczka-Cyriac, M. (2010) Iron isotope fractionation mechanisms of silicate weathering and iron cycling by plants. Ph.D. thesis, ETH Zurich.

Krabbenhöft A., Fietzke J., Eisenhauer A., Liebetrau V., Böhm F. and Vollstaedt H. (2009) Determination of radiogenic and stable strontium isotope ratios (^{87}Sr/^{86}Sr; $\delta^{88/86}$Sr) by thermal ionisation mass spectrometry applying an ^{87}Sr/^{84}Sr double spike. *J. Anal. Atom. Spectrom.* **24**, 1267–1271.

Lasaga A. C. (1994) Chemical weathering rate laws and global geochemical cycles. *Geochim. Cosmochim. Acta* **58**, 2361–2386.

Lemarchand D., Wasserburg G. J. and Papanastassiou D. A. (2004) Rate-controlled calcium isotope fractionation in synthetic calcite. *Geochim. Cosmochim. Acta* **68**, 4665–4678.

Lemarchand E., Schott J. and Gaillardet J. (2005) Boron isotope fractionation related to boron sorption on humic acid and the structure of surface complexes formed. *Geochim. Cosmochim. Acta* **69**, 3519–3533.

Ludwig W., Amiotte-Suchet P. and Probst J.-L. (1999) Enhanced chemical weathering of rocks during the last glacial maximum: a sink for atmospheric CO_2? *Chem. Geol.* **159**, 147–161.

Marshall B. D. and DePaolo D. J. (1982) Precise age determinations and petrogenic studies using the K–Ca method. *Geochim. Cosmochim. Acta* **46**, 2537–2545.

Mavris C., Egli M., Plötze M., Blum J. D., Mirabella A., Giaccai D. and Haeberli W. (2010) Initial stages of weathering and soil formation in the Morteratsch proglacial area (Upper Engadine, Switzerland). *Geoderma* **155**, 359–371.

Meybeck M. (1987) Global chemical weathering of surficial rocks estimated from river dissolved loads. *Am. J. Sci.* **287**, 401–428.

Mikutta C., Wiederhold J. G., Cirpka O. A., Hofstetter T. B., Bourdon B. and Von Gunten U. (2009) Iron isotope fractionation and atom exchange during sorption of ferrous iron to mineral surfaces. *Geochim. Cosmochim. Acta* **73**, 1795–1812.

Miller W. R. and Drever J. I. (1977) Chemical weathering and related controls on surface water chemistry in the Absaroka Mountains, Wyoming. *Geochim. Cosmochim. Acta* **41**, 1693–1702.

Nezat C. A., Blum J. D., Yanai R. D. and Hamburg S. P. (2007) A sequential extraction to determine the distribution of apatite in granitoid soil mineral pools with application to weathering at the Hubbard Brook Experimental Forest, NH, USA. *Appl. Geochem.* **22**, 2406–2421.

Nezat C. A., Blum J. D., Yanai R. D. and Park B. B. (2008) Mineral sources of calcium and phosphorus in soils of the northeastern United States. *Soil Sci. Soc. Am. J.* **72**, 1786–1794.

Oliva P., Dupré B., Martin F. and Viers J. (2004) The role of trace minerals in chemical weathering in a high-elevation granitic watershed (Estibère, France): Chemical and mineralogical evidence. *Geochim. Cosmochim. Acta* **68**, 2223–2244.

Oliva P., Viers J. and Dupré B. (2003) Chemical weathering in granitic environments. *Chem. Geol.* **202**, 225–256.

Page B. D., Bullen T. D. and Mitchell M. J. (2008) Influences of calcium availability and tree species on Ca isotope fractionation in soil and vegetation. *Biogeochemistry* **88**, 1–13.

Palmer M. R. and Edmond J. M. (1992) Controls over the strontium isotope composition of river water. *Geochim. Cosmochim. Acta* **56**, 2099–2111.

Poszwa A., Dambrine E., Pollier B. and Atteia O. (2000) A comparison between Ca and Sr cycling in forest ecosystems. *Plant Soil* **225**, 299–310.

Rauret G., López-Sánchez J.-F., Sahuquillo A., Barahona E., Lachica M., Ure A. M., Davidson C. M., Gomez A., Lück D., Bacon J., Yli-Halla M., Muntau H. and Quevauviller P. (2000) Application of a modified BCR sequential extraction (three-step) procedure for the determination of extractable trace metal contents in a sewage sludge amended soil reference material (CRM 483), complemented by a three-year stability study of acetic acid and EDTA extractable metal content. *J. Environ. Monitor.* **2**, 228–233.

Richter F. M., Rowley D. B. and DePaolo D. J. (1992) Sr isotope evolution of seawater: the role of tectonics. *Earth Planet. Sci. Lett.* **109**, 11–23.

Rudge J. F., Reynolds B. C. and Bourdon B. (2009) The double spike toolbox. *Chem. Geol.* **265**, 420–431.

Russell W. A. and Papanastassiou D. A. (1978) Calcium isotope fractionation in ion exchange chromatography. *Anal. Chem.* **50**, 1151–1154.

Schaltegger U. (1994) Unravelling the pre-Mesozoic history of Aar and Gotthard massifs (Central Alps) by isotopic dating – a review. *Schweiz. Mineral. Petrog. Mitt.* **74**, 41–51.

Schiller M., Bizzarro M., Baker J. A. (2007) Development of precise and accurate magnesium isotope measurements by multiple-collector inductively coupled plasma mass spectrometry. Workshop on the chronology of meteorites and the early solar system, Kauai, Hawaii, pp. 149–150.

Schmitt A.-D., Chabaux F. and Stille P. (2003) The calcium riverine and hydrothermal isotopic fluxes and the oceanic calcium mass balance. *Earth Planet. Sci. Lett.* **6731**, 1–16.

Siebert C., Nägler T.F., Kramers J.D. (2001) Determination of molybdenum isotope fractionation by double-spike multicollector inductively coupled plasma mass spectrometry. *Geochem. Geophys. Geosyst.* **2**.

Simon J. I., DePaolo D. J. and Moynier F. (2009) Calcium isotope composition of meteorites, Earth and Mars. *Astrophys. J.* **702**, 707–715.

Skulan J., DePaolo D. J. and Owens T. L. (1997) Biological control of calcium isotopic abundances in the global calcium cycle. *Geochim. Cosmochim. Acta* **61**, 2505–2510.

Smittenberg R. H., Hajdas I., Wacker L. and Bernasconi S. M. (2009) Soil organic geochemistry and carbon dynamics of an alpine chronosequence. *Geochim. Cosmochim. Acta* **73**, A1242.

Steiger R. H. and Jäger E. (1977) Subcommission on Geochronology – convention on use of decay constants in geochronology and cosmochronology. *Earth Planet. Sci. Lett.* **36**, 359–362.

Tipper E. T., Gaillardet J., Galy A., Louvat P., Bickle M. J. and Campas F. (2010) Calcium isotope ratios in the world's largest rivers: a constraint on the maximum imbalance of oceanic calcium fluxes. *Global Biogeochem. Cycles* **24**, GB3019.

Tipper E. T., Galy A. and Bickle M. J. (2006) Riverine evidence for a fractionated reservoir of Ca and Mg on the continents: implications for the oceanic Ca cycle. *Earth Planet. Sci. Lett.* **247**, 267–279.

Tipper E. T., Galy A. and Bickle M. J. (2008) Calcium and magnesium isotope systematics in rivers draining the Himalaya–Tibetan–Plateau region: lithological or fractionation control? *Geochim. Cosmochim. Acta* **72**, 1057–1075.

Valsami-Jones E., Ragnarsdottir K. V., Putnis A., Bosbach D., Kemp A. J. and Cressey G. (1998) The dissolution of apatite in the presence of aqueous metal cations at pH 2–7. *Chem. Geol.* **151**, 215–233.

VAW, 2005. Gletscherberichte (1881–2002) 'Die Gletscher der Schweizer Alpen', Jahrbücher der Glaziologischen Kommission der Schweizerischen Akademie der Naturwissenschaften (SANW) durch die Versuchsanstalt für Wasserbau, Hydrologie und Glaziologie (VAW) (http://glaziology.ethz.ch/swiss-glaciers/). ETH Zürich.

Verbunt M., Gurtz J., Jasper K., Lang H., Warmerdam P. and Zappa M. (2003) The hydrological role of snow and glaciers in alpine river basins and their distributed modeling. *J. Hydrol.* **282**, 36–55.

Walker J. C. G., Hays P. B. and Kasting J. F. (1981) A negative feedback mechanism for the long term stabilization of Earth's surface temperature. *J. Geophys. Res.* **86**, 9776–9782.

White A. F. and Blum A. E. (1995) Effects of climate on chemical weathering in watersheds. *Geochim. Cosmochim. Acta* **59**, 1729–1747.

White A. F., Bullen T. D., Vivit V., Schulz M. S. and Clow D. W. (1999) The role of disseminated calcite in the chemical weathering of granitoid rocks. *Geochim. Cosmochim. Acta* **63**, 1939–1953.

Wiederhold J. G., Teutsch N., Kraemer S. M., Halliday A. N. and Kretzschmar R. (2007) Iron isotope fractionation in oxic soils by mineral weathering and podzolization. *Geochim. Cosmochim. Acta* **71**, 5821–5833.

Wiegand B. A., Chadwick O. A., Vitousek P. M. and Wooden J. L. (2005) Ca cycling and isotopic fluxes in forested ecosystems in Hawaii. *Geophys. Res. Lett.* **32**, L11404.

WRB (2006) World Reference Base for Soil Resources 2006 – a framework for International Classification, Correlation and Communication. No. 103. Food and Agriculture Organization of the United Nations, Rome, Italy.

Associate editor: Derek Vance